Title

Dentate nucleus iron deposition is a potential biomarker for tremor-dominant Parkinson's disease.

Journal

NMR in biomedicine, 30(4)

ISSN

0952-3480

Authors

He, Naying
Huang, Pei
Ling, Huawei
et al.

Publication Date

2017-04-01

DOI

10.1002/nbm.3554

Peer reviewed

HHS Public Access

Author manuscript

NMR Biomed. Author manuscript; available in PMC 2018 April 01.

Published in final edited form as:

NMR Biomed. 2017 April ; 30(4): . doi:10.1002/nbm.3554.

Dentate nucleus iron deposition is a potential biomarker for tremor-dominant Parkinson's disease

Naying He[1,*], **Pei Huang**[2,*], **Huawei Ling**[1], **Jason Langley**[3], **Chunlei Liu**[4,5], **Bei Ding**[1], **Juan Huang**[1], **Hongmin Xu**[1], **Yong Zhang**[6], **Zhongping Zhang**[6], **Xiaoping Hu**[3], **Shengdi Chen**[2,**], and **Fuhua Yan**[1,**]

[1]Department of Radiology, Ruijin Hospital, Shanghai Jiao Tong University School of Medicine, Shanghai 200025, China

[2]Department of Neurology and Institute of Neurology, Ruijin Hospital, Shanghai Jiao Tong University School of Medicine, Shanghai 200025, China

[3]Wallace H. Coulter Department of Biomedical Engineering, Georgia Institute of Technology and Emory University, Atlanta, GA 30322, USA

[4]Brain Imaging and Analysis Center, Duke University Medical Center, Durham, NC 27710, USA

[5]Department of Radiology, Duke University Medical Center, Durham, NC 27710, USA

[6]MR Research, GE Healthcare, Shanghai, China

Abstract

Parkinson disease (PD) is a heterogeneous neurodegenerative disorder with variable clinicopathologic phenotypes and underlying neuropathologic mechanisms. Each clinical phenotype has a unique set of motor symptoms. Tremor is the most frequent initial motor symptom of PD and is the most difficult symptom to treat. The dentate nucleus (DN) is a deep iron rich nucleus in the cerebellum and may be involved in PD tremor. In this study, we test the hypothesis that DN iron may be elevated in tremor dominant PD patients using quantitative susceptibility mapping. Forty-three patients with PD [19 tremor dominant (TD)/24 akinetic-rigid dominant (AR)] and 48 healthy gender- and age-matched controls were recruited. Multi-echo gradient echo data were collected for each subject on a 3.0 T MR system. Inter-group susceptibility differences in bilateral DN were investigated and correlations of clinical features with susceptibility were also examined. In contrast to the AR group, the TD group was found to have increased susceptibility in the bilateral DN, when compared to healthy controls. In addition, susceptibility was positively correlated with tremor score in drug naive PD patients. These findings indicate that iron load within DN may make an important contribution to motor phenotypes in PD. Moreover, our results suggest that TD and AR phenotypes of PD can be differentiated on the basis of the susceptibility of the DN at least on the group level.

**Correspondence to: Fuhua Yan, Department of Radiology, Ruijin Hospital, Shanghai Jiao Tong University School of Medicine, No. 197 Ruijin Er Road, Shanghai, 200025, China. anfuhua@yahoo.com. Shengdi Chen, Department of Neurology and Institute of Neurology, Ruijin Hospital, Shanghai Jiao Tong University School of Medicine, Shanghai 200025, China. chen_sd@medmail.com.cn.

*Both authors contributed equally to this work

CONFLICT OF INTEREST

All authors declare no biomedical financial interests or potential conflicts of interest.

Keywords

Parkinson's disease; tremor dominant phenotype; akinetic-rigid dominant phenotype; quantitative susceptibility mapping; iron deposition

INTRODUCTION

It is increasingly evident that Parkinson disease (PD) is not a single entity but rather a heterogeneous neurodegenerative disorder with variable clinicopathologic phenotypes and underlying neuropathologic mechanisms[1, 2]. Each PD phenotype is marked by distinct dominant motor symptoms including tremor and akinetic rigidity[3]. Based on these symptoms, PD is grouped into three motor phenotypes, tremor dominant (TD), akinetic rigidity (AR) dominant, and mixed group[4]. Currently, these phenotypes are categorized using clinical scales, which are highly subjective. In addition, once patients become symptomatic, significant degeneration of sub-cortical grey matter structures has already occurred[5].

Current therapies only treat symptoms and do not reverse the degeneration in sub-cortical grey matter structures. This is particularly true for the treatment of PD tremor, which does not respond to dopamine replacement therapy as well as AR [6, 7]. Hence, identification of subtype-specific biomarkers to categorize the PD phenotypes will remove this subjectivity and lead to a more holistic understanding of PD pathogenesis, which may give additional insights into prodromal PD, disease progression, and clinical prognosis.

Deep brain stimulation (DBS) of subthalamic nucleus (STN) and ventral intermediate nucleus (VIM) has been shown to effectively reduce PD tremor severity[8, 9]. STN and VIM are structurally and functionally connected to the motor cortex through the dentatorubro-thalamic tract and the cerebello-thalamo-cortical (CTC) circuit, which play an important role in PD tremor[10–12]. Given that the dentate nucleus (DN) is the origin of the dentatorubro-thalamic tract and lies in the CTC circuit, it could play an active role in PD tremor. However, the role of DN in the pathophysiology of PD tremor has not been elucidated.

DN is an iron rich grey matter nucleus in the cerebellum. Iron deposition has been measured in other sub-cortical brain structures including the substantia nigra (SN), red nucleus, and basal ganglia[13–17] in PD using different MRI contrasts including R_2*[14, 15, 18, 19] and quantitative susceptibility mapping (QSM) [13, 20]. However, the amount of iron deposited in the DN after PD onset is unclear. In the aforementioned sub-cortical structures, increased iron load leads to free radical production, oxidative stress, and perhaps neuronal death[21]. Given the relationship between iron and neuronal death in these structures[21], it is not surprising that iron content has been found to correlate with clinical measures of disease severity[13].

Iron containing proteins in the brain are paramagnetic[14, 18, 19] and increase magnetic susceptibility. For sub-cortical structures with high iron concentrations, there should be large differences in susceptibility between these structures and background tissues, which can be taken advantage of to clearly delineate the outlines of these structures *in vivo*[22]. QSM

estimates relative susceptibility differences between tissues by modeling magnetic field inhomogeneities as magnetic dipoles then inverting the dipole field[23]. In contrast with conventional methods mapping the transverse relaxation rate (R_2^*), QSM provides a better contrast to noise ratio and clearer delineation of deep grey matter structures, and is less affected by bulk field inhomogeneity[24–26]. QSM has been applied to quantitatively evaluate relative iron concentrations in multiple sclerosis[27, 28], Alzheimer's disease[29], and normal aging[25]. In PD, QSM has revealed elevated iron levels in SN as defined in T_2 weighted contrasts[13, 20, 30].

Iron accumulation in DN after onset of PD may affect the CTC circuit and allow for differentiation of PD phenotypes. In this study, we use QSM to establish a relationship between susceptibility (a surrogate marker for relative iron concentration in deep brain nuclei) in DN and PD motor phenotype. Furthermore, we measure the correlation between susceptibility in the bilateral DN and clinical features. This is the first QSM study focusing on the DN to ascertain whether DN iron might be a biomarker for tremor dominant PD patients.

MATERIALS AND METHODS

Participants

Forty-three right-handed PD patients (age 63.7±6.9 years; male/female 19/24) were recruited from the movement disorder outpatient clinic in Ruijin Hospital, Shanghai Jiao Tong University School of Medicine. PD diagnosis was confirmed by a movement disorder specialist (C.S.D) according to the United Kingdom Parkinson's Disease Society Brain Bank criteria[31]. Demographic information including gender, age, and education was collected for each patient. Disease severity was evaluated using Hoehn & Yahr (H&Y)[32] staging, and motor disability of PD was assessed with the motor portion of the Unified Parkinson's Disease Rating Scale (UPDRS)-III[33]. All PD subjects completed the non-motor symptoms (NMS) questionnaire, a validated tool for detecting NMS[34, 35]. For each subject in the PD group, olfactory dysfunction was evaluated using a validated version of the 16 item smell identification test from Sniffin' Sticks (SS-16)[36].

Lateral impairment was determined and the side of initial PD motor symptoms was recorded for each PD patient by the movement disorders specialist (C.S.D). Twenty-three subjects displayed initial impairment on the left side and 20 subjects showed initial impairment on the right side.

The PD patients were classified into three subgroups, TD group, AR group, and mixed group following the methods used in a prior study[37]. These classifications were derived from the UPDRS-III score. Briefly, subgroups were identified based on the ratio of each patient's UPDRS-III tremor score (sum of items 20 and 21 in UPDRS-III divided by 4) to their mean UPDRS akinetic/rigid score (sum of items 22–27 and 31 in UPDRS-III divided by 15), with a ratio greater than 1.0 being defined as TD, a ratio less than 0.80 being assigned AR dominant, and a ratio between 0.80 and 1.0 being mixed-type[38]. In this study, only TD and AR patients were included. Nineteen (TD:13; AR:6) of the 43 PD patients were drug naive (either no previous levodopa exposure or levodopa exposure less than 2 weeks and no

levodopa within 4 weeks prior to study entry). For the other 24 PD subjects (TD:6; AR:18), all the clinical scaling and MRI scanning were carried out at least 12 h after the last dose of dopaminergic medication.

Exclusion criteria were as follows: (1) symptoms or signs of secondary or atypical parkinsonism[39–41]; (2) Mini-Mental State Exam (MMSE) score less than 24; (3) a history of cerebrovascular disease, seizures, brain surgery, brain tumor, moderate-to-severe head trauma or hydrocephalus, and any psychiatric disorders; (4) treatment with antipsychotic or with any other drug possibly affecting clinical evaluation.

Forty-eight gender- and age-matched right handed healthy controls (age 61.7±6.5 years; male/female 21/27) were recruited from the local community by advertisements. All of them had normal movement function and neurological status, absence of neurological or psychiatric disease, and a MMSE score equal to or greater than 24. The current study was approved by local ethical committees and data were collected between June 2014 and June 2015. All the subjects provided written informed consent.

Data Acquisition

MRI scanning was performed on a 3.0-Tesla MR system (Signa HDxt; GE Healthcare, Milwaukee, WI) equipped with an eight-channel phased array head coil. For each participant, foam padding was applied to prevent head movement and earplugs were provided to reduce scanner noise. Conventional MR images, including T_1-weighted and T_2-weighted fluid-attenuated inversion recovery (FLAIR) images were acquired for screening of cerebrovascular diseases and space-occupying lesions in the basal ganglia and mesencephalon. Thereafter, a three-dimensional multi-echo gradient echo (GRE) sequence was utilized to obtain T_2^*-weighted images. Imaging parameters for the multiecho GRE sequence were as follows: repetition time (TR), 59.3 msec; number of echoes, sixteen; first echo time, 2.7 msec; echo time spacing, 2.9 msec; bandwidth, 62.5kHz (488.28Hz/pixel); flip angle, 12°; field of view, 22 cm; matrix size, 256×256; resolution $0.86\times0.86\times1.0mm^3$; acceleration factor 2 (approximately 70% of k-space was sampled); slices, 136; and a total acquisition time of 10 minutes 42 seconds. The whole brain was covered for all MR scans including the multi-echo GRE sequence, which was run on the axial plane parallel to the anterior commissure-posterior commissure line.

Image Pre-processing

Image processing was performed as described in previous studies[24]. The complex images were obtained directly from the scanner and were reconstructed with a parallel imaging reconstruction algorithm, ASSET, provided by the manufacturer (GE Healthcare). The ASSET algorithm used the complex coil sensitivity maps acquired separately to reconstruct the underdamped GRE data. As a result, phase in coil sensitivity was removed during the reconstruction. Phase was unwrapped after image reconstruction[42]. The background phase was then removed with the spherical mean value method using a filter radius of 8 pixels[43]. Finally, susceptibility maps were derived from the frequency map of brain tissue using an improved LSQR method (iLSQR)[24, 44] and Laplace filtering with a threshold of 0.04 as a

truncation value. All image processing was performed in MATLAB (the Math-Works, Inc., Natick, MA, USA) using home-made scripts.

Image Analysis

Previous studies have shown that cerebrospinal fluid (CSF) regions tend to be heterogeneous due to various causes such as flow, partial volume effects, and vasculature[25, 26, 45]. In addition, white matter is not a suitable reference because white matter abnormalities have been reported in PD[46, 47]. Hence, susceptibility values obtained from QSM were directly used for comparison without referencing any selected structures; they were thus inherently referenced to the mean susceptibility of the whole brain due to the setting of Larmor frequency to the mean. Furthermore, since mean susceptibility of the whole brain contains all contributing sources, it is less likely biased by variations in any single structure, thus providing the most stable available reference. Due to the unresolved issue of QSM normalization, we have included the results obtained by normalizing the QSM data to CSF in the supplementary materials section.

Bilateral DNs (as shown in Figure 1) were drawn manually on the susceptibility maps using MRIcro software (www.mricro.com) by two neuroradiologists who were blinded to the diagnosis of each subject. The QSM values for bilateral DNs were obtained from all visible sections. In addition, the volume of the final set of ROIs was determined by multiplying the sum of voxels within the entire structure by the size of each voxel ($0.86\times0.86\times1.0mm^3$). The inter-rater reliability for manual DN segmentation was assessed (see the statistical section for further details). If there was “excellent agreement” between the raters, the voxels identified by both raters, calculated using MRIcro software, were used as ROIs for subsequent analyses. The same set of DN ROIs was used to determine R_2^* values in DN. R_2^* values in DN were calculated using a monoexponential model:

$$y=\alpha e^{-R_2^* TE}$$

where α denoted a fitting constant.

Statistical Analysis

An independent two-sample t-test was performed to compare age, education, and MMSE between the PD and HC groups. A Chi-square test was performed to assess the inter-group gender heterogeneity between the groups.

To address the inter-rater reliability of the two neuroradiologists segmenting DNs on susceptibility maps, absolute intra-class correlation coefficients (ICC) were calculated[48]. ICC provides a measure for agreement between the raters for segmentation of the ROIs. An ICC above 0.81 was defined as excellent agreement, 0.61–0.80 as good agreement, 0.41–0.60 as moderate agreement, 0.21–0.40 as fair agreement, and 0.20 or less as poor agreement.

Bilateral susceptibility, R_2^* value, and volume of the DN in the PD subgroups were compared with pertinent mean values in control group using covariance (ANCOVA)

analysis, and Bonferroni correction was used for comparison between multiple groups (p-value threshold for significance: 0.025). To investigate the correlation of QSM and R_2^* values in the bilateral DN with clinical features (duration of Parkinson's disease, UPDRS-III score, tremor score, akinetic-rigidity score, MMSE, NMS-Quest, and SS-16), partial correlation analysis was performed with gender, age, and education as covariates in drug naive PD patients (13 patients from TD group and 6 patients from AR group), as there would be potential contamination of the clinical scores of PD patients in medication "off-state"[49, 50]. Bonferroni correction was adjusted for multiple comparisons in the correlation analyses (p-value threshold for significance: 0.00357). All statistical analyses were performed using SPSS software (ver. 18.0; SPSS, Inc., Chicago, IL, USA). The threshold of statistical significance was set to $p<0.05$, except for the Bonferroni correction.

RESULTS

Demographic and Clinical Data Analyses

No significant differences were seen in gender ($p=0.97$), age ($p=0.89$), education ($p=0.36$), and MMSE scores ($p=0.66$) between PD and control groups. No significant differences were found between the TD and AR groups in age ($p=0.43$), education ($p=0.55$), MMSE ($p=0.51$), and ss-16 ($p=0.06$). The AR group has significantly longer illness duration (AR: 7.0±4.5 ; TD:4.2±3.9 ; $p=0.04$), higher UPDRS-III scores (AR:26.8±13.1; TD:16.1±7.3; $p=0.002$), higher NMS-Quest scores (AR:7.3±4.7; TD:3.6±3.3; $p=0.006$) than the TD group. Patients with TD exhibited higher TD score than patients with AR (TD:3.8±2.2; AR: 1.1±1.4; $p<0.001$) and patients with AR had higher AR score than patients with TD (AR: 20.0±10.3; TD: 8.7±3.8; $p<0.001$), consistent with clinical manifestations of each subtype. All the demographic and clinical data for PD subgroups and HCs group are shown in Table 1.

Volume results in DN

DN volumes were manually traced on QSM maps by two neuroradiologists blinded to the status of each subject. ICCs for absolute agreement between raters with respect to bilateral DN segmentation were greater than 0.81 (ipsilateral DN: ICC=0.92; contralateral DN: ICC=0.91), indicating excellent inter-rater agreement. No significant difference in DN volume was found between PD and control groups (ipsilateral: $p=0.13$; contralateral: $p=0.13$). Interestingly, no significant differences were observed in ipsilateral and contralateral DN volume between healthy controls and TD patients (ipsilateral: $p=0.14$; contralateral: $p=0.25$) or AR patients (ipsilateral: $p=0.35$; contralateral: $p=0.22$). These results are summarized in Table 2. In the rest of this paper, ipsilateral and contralateral denote DN volumes ipsilateral and contralateral to the side showing initial motor symptoms in PD patients.

Susceptibility in DN

Susceptibility in the bilateral DN of the entire PD group showed no significant difference when compared with the healthy control group (ipsilateral: $p=0.40$; contralateral: $p=0.32$). The AR group has similar bilateral DN susceptibility values as healthy controls (ipsilateral: $p=0.35$; contralateral: $p=0.53$). In contrast, the TD subgroup was found to have greater

susceptibility values in both ipsilateral (p=0.02) and contralateral (p=0.02) DN, indicating elevated iron levels in the DN of individuals with TD phenotype. After further comparison between TD and AR groups, we found that DN susceptibility values of TD group were significantly higher than that of AR group (ipsilateral: p=0.004; contralateral: p=0.01). For the details see Table 2 and Figure 2.

R_2^* in DN

There were no significant differences between bilateral DN R_2^* of TD group (ipsilateral: p=0.06; contralateral: p=0.10) or AR group (ipsilateral: p=0.30: contralateral: p=0.63) and R_2^* in DN of control group.

Correlation Analysis

A partial correlation analysis was performed to assess the dependence of susceptibility in DN on clinical features. The ipsilateral DN susceptibility was significantly correlated with tremor score (r=0.69; p=0.003) in drug naive PD patients after correcting for multiple comparisons, while the susceptibility values in contralateral DN showed a moderate trend with tremor score in drug naive PD patients (r=0.60; p=0.01). In order to investigate the relationship between DN susceptibility and clinical features in the drug naive TD cohort (n=13), we performed a partial correlation analysis with gender, age, and education as covariates. Trends were seen between bilateral DN susceptibility and tremor score (ipsilateral: r=0.61, p=0.06; contralateral: r=0.57, p=0.09) as well as between bilateral DN susceptibility and disease duration (ipsilateral: r=0.73, p=0.02; contralateral: r=0.70, p=0.03) in the 13 drug-naive TD patients. No other significant correlation was seen between susceptibility in DN and clinical features after multiple comparison correction. For the details see Table 3 and Figure 3. There were no significant correlations between DN R_2^* values and clinical features in drug naive PD group.

DISCUSSION

This study assessed the dependence of motor phenotype on iron deposition by comparing susceptibility of bilateral DN in TD and AR groups to that of a healthy control group. DN iron deposition in these PD phenotype**s** has not been previously reported. In contrast to the AR group, we found increased susceptibility values in the bilateral DN of the TD group when compared to healthy controls. In addition, bilateral DN susceptibility was positively correlated with tremor score in drug naive PD patients. These findings suggest that iron load within DN may play a role in the development of PD motor symptoms. Moreover, our results suggest that TD and AR phenotypes can be differentiated on the basis of the susceptibility in DN at least on the group level.

PD tremor is one of the primary symptoms of PD and is the most difficult symptom to treat since dopamine replacement therapy is not as effective as a treatment in TD as in other PD phenotypes[6, 7]. The ineffectiveness of dopamine replacement therapy could be due to TD patients having less dopaminergic neuronal loss in the substantia pars compacta and locus coeruleus than other PD phenotypes[51, 52]. In lieu of dopamine replacement therapy, DBS of VIM or STN has been found to be an effective treatment for TD patients and has been

shown to normalize cerebellar activation[53, 54]. Both nuclei are key to the function of CTC, which is the major efferent of cerebellum[55].

Previous positron emission tomography (PET) studies have shown that PD tremor is mediated by CTC pathways and found correlations with increased metabolic activity in DN/cerebellum and PD tremor[56]. Other metabolic studies found a reduction of GABA receptors in DN of essential tremor patients, which shares common functional pathways with PD tremor[57]. These results accord well with fMRI studies, which have detected hyperactivity in DN in TD phenotype[58, 59]. In the current study, we found increased susceptibility (relative iron concentration) within bilateral DN of TD when compared with AR and HC groups. Interestingly, the DN susceptibility values were positively correlated with tremor score of drug naive PD patients. Taken together with the previously reported results, we speculate that iron deposition interrupts normal CTC function.

The specific mechanism underlying increased iron deposition in TD is not clear but oxidative stress induced by increased iron load is known to cause neuronal death by altering the valence state between ferrous (Fe2+) and ferric (Fe3+) forms of iron[60]. It is possible that there is a reduction of DN neurons due to elevated iron levels and the remaining DN neurons increase their functional activity to compensate for this loss. This may affect the functional connectivity between the cerebellum and basal ganglia and disrupt CTC function. Further parkinsonian phenotype specific DN histological studies are needed to verify this conjecture but this explanation accords well with functional and metabolic studies[56, 58].

No difference in DN R_2^* values was seen between TD or AR groups and the control group. However, increased susceptibility values in DN of the TD group were observed, indicating elevated DN iron levels in this group. The failure to detect significant R_2* difference could be caused by the lower contrast-to-noise ratio in R_2* values. Alternatively, since R_2^* is sensitive to larger sized iron particles[61, 62], it is also possible that the increased iron deposited in DN is comprised of smaller sized particles. These iron particles may be in the molecular form and not bound with proteins. The increase in these particles could potentiate a state of neuron inflammation, drive additional neuronal loss, and exacerbate tremor symptoms[63].

In contrast to TD phenotype, there is increased dopaminergic neuronal loss in substantia nigra pars compacta and basal ganglia of AR phenotype[64, 65]. Both structures lie outside the CTC circuit, and in the AR phenotype, tremor symptoms are not as pronounced as in TD phenotype. Thus, we expect less disruption of the CTC circuit in AR patients than in TD patients. This agrees well with the current finding of no increase in iron content in bilateral DN of the AR group. Our result may indicate that there is little to no disruption in CTC functionality in AR group from DN iron deposition.

Prior work examining iron load in DN did not find significant changes in SWI signal intensity in PD when compared to controls[66]. In comparison to the current study, the previous study did not distinguish PD phenotype. We found similar iron concentrations in AR group and healthy controls, while the TD group showed increased iron deposition in

bilateral DN when compared to controls. Our results suggest that DN iron level is not a general feature of PD but is a phenotype specific feature.

In this study, we performed correlation analyses between bilateral DN susceptibility and clinical features in the drug naive PD cohort instead of the cohort of all PD patients, as the clinical scores of the medication “off-state” PD patients would still be potentially affected by dopamine replacement treatment[49, 50]. There are two known types of dopamine therapy duration with respect to motor responses, short and long[49, 50]. The long-duration benefits of Levodopa last approximately one to two weeks[50]. Theoretically there may be residual effects of dopamine replacement therapy in PD patients in the off-medication state, which may potentially affect motor symptoms and the resulting clinical scores. Through the partial correlation analyses, we found that DN susceptibility was positively correlated with tremor score in drug naive PD patients, likely indicating that susceptibility in DN is a potential marker for the severity of PD tremor. We speculate that the amount of DN iron deposition can predict the severity of tremor symptoms in PD patients and may give a more quantitative measure than UPDRS-III score for the evaluation of the efficacy of future tremor treatments.

There are some limitations in the current study. Firstly, bilateral DN regions were manually delineated rather than using automatic or semi-automatic methods. Manual delineation is time-consuming and may cause potential subjective bias, but reliability of this segmentation was tested with agreement between raters (ICC), and the ICC values are high (more than 0.81) in this study. Second, the results should be interpreted with caution for lack of histological confirmation and limited sample size, and longitudinal investigation is warranted in the future.

Overall, the results of the present study highlight different DN iron loads between TD and AR phenotypes. These results provide a better understanding of subtype-specific diagnostic biomarkers and provide insights into mechanisms of neurodegeneration as well as improve future epidemiologic and therapeutic clinical trial designs.

Acknowledgments

The study was supported in part through State Key Clinical Department of Medical Imaging, National Natural Science Fund (81430022, 81371407), and SHSMU-ION Research Center for Brain Disorders. CL is supported in part by the National Institutes of Health through grants NIMH R01MH096979 and NINDS R01NS079653, and by the National Natural Science Foundation of China through grant 81428013. XH and JL are supported in part by the Michael J. Fox Foundation (MJF 10854). The authors acknowledge Dr. Qian Sun and Dr. Binying Li for sharing part of their clinical database for evaluation for this study. The authors wish to thank all patients and healthy control subjects who participated in this study.

References

1. Thenganatt MA, Jankovic J. Parkinson disease subtypes. JAMA neurology. 2014; 71:499–504. [PubMed: 24514863]
2. Marras C, Rochon P, Lang AE. Predicting motor decline and disability in Parkinson disease: a systematic review. Archives of neurology. 2002; 59:1724–1728. [PubMed: 12433259]
3. Lees AJ, Hardy J, Revesz T. Parkinson’s disease. Lancet. 2009; 373:2055–2066. [PubMed: 19524782]
4. Rajput AH, Voll A, Rajput ML, Robinson CA, Rajput A. Course in Parkinson disease subtypes: A 39-year clinicopathologic study. Neurology. 2009; 73:206–212. [PubMed: 19620608]

5. Fearnley JM, Lees AJ. Ageing and Parkinson's disease: substantia nigra regional selectivity. Brain. 1991; 114(Pt 5):2283–2301. [PubMed: 1933245]
6. Koller WC, Busenbark K, Miner K. The relationship of essential tremor to other movement disorders: report on 678 patients. Essential Tremor Study Group. Ann Neurol. 1994; 35:717–723. [PubMed: 8210229]
7. Fishman PS. Paradoxical aspects of parkinsonian tremor. Movement disorders : official journal of the Movement Disorder Society. 2008; 23:168–173. [PubMed: 17973325]
8. Coenen VA, Allert N, Paus S, Kronenburger M, Urbach H, Madler B. Modulation of the cerebello-thalamo-cortical network in thalamic deep brain stimulation for tremor: a diffusion tensor imaging study. Neurosurgery. 2014; 75:657–669. discussion 669–670. [PubMed: 25161000]
9. Mehanna R, Lai EC. Deep brain stimulation in Parkinson's disease. Translational neurodegeneration. 2013; 2:22. [PubMed: 24245947]
10. Ni Z, Pinto AD, Lang AE, Chen R. Involvement of the cerebellothalamocortical pathway in Parkinson disease. Ann Neurol. 2010; 68:816–824. [PubMed: 21194152]
11. Helmich RC, Janssen MJ, Oyen WJ, Bloem BR, Toni I. Pallidal dysfunction drives a cerebellothalamic circuit into Parkinson tremor. Ann Neurol. 2011; 69:269–281. [PubMed: 21387372]
12. Lewis MM, Du G, Sen S, Kawaguchi A, Truong Y, Lee S, Mailman RB, Huang X. Differential involvement of striato- and cerebello-thalamo-cortical pathways in tremor- and akinetic/rigid-predominant Parkinson's disease. Neuroscience. 2011; 177:230–239. [PubMed: 21211551]
13. He N, Ling H, Ding B, Huang J, Zhang Y, Zhang Z, Liu C, Chen K, Yan F. Region-specific disturbed iron distribution in early idiopathic Parkinson's disease measured by quantitative susceptibility mapping. Hum Brain Mapp. 2015; 36:4407–4420. [PubMed: 26249218]
14. Gorell JM, Ordidge RJ, Brown GG, Deniau JC, Buderer NM, Helpern JA. Increased iron-related MRI contrast in the substantia nigra in Parkinson's disease. Neurology. 1995; 45:1138–1143. [PubMed: 7783878]
15. Lewis MM, Du G, Kidacki M, Patel N, Shaffer ML, Mailman RB, Huang X. Higher iron in the red nucleus marks Parkinson's dyskinesia. Neurobiol Aging. 2013; 34:1497–1503. [PubMed: 23177595]
16. Wallis LI, Paley MNJ, Graham JM, Gruenewald RA, Wignall EL, Joy HM, Griffiths PD. MRI Assessment of Basal Ganglia Iron Deposition in Parkinson's Disease. Journal of Magnetic Resonance Imaging. 2008; 28:1061–1067. [PubMed: 18972346]
17. Zhang J, Zhang Y, Wang J, Cai P, Luo C, Qian Z, Dai Y, Feng H. Characterizing iron deposition in Parkinson's disease using susceptibility-weighted imaging: an in vivo MR study. Brain Res. 2010; 1330:124–130. [PubMed: 20303339]
18. Martin WR, Wieler M, Gee M. Midbrain iron content in early Parkinson disease: a potential biomarker of disease status. Neurology. 2008; 70:1411–1417. [PubMed: 18172063]
19. Peran P, Cherubini A, Assogna F, Piras F, Quattrocchi C, Peppe A, Celsis P, Rascol O, Demonet JF, Stefani A, Pierantozzi M, Pontieri FE, Caltagirone C, Spalletta G, Sabatini U. Magnetic resonance imaging markers of Parkinson's disease nigrostriatal signature. Brain. 2010; 133:3423–3433. [PubMed: 20736190]
20. Lotfipour AK, Wharton S, Schwarz ST, Gontu V, Schafer A, Peters AM, Bowtell RW, Auer DP, Gowland PA, Bajaj NP. High resolution magnetic susceptibility mapping of the substantia nigra in Parkinson's disease. Journal of magnetic resonance imaging : JMRI. 2012; 35:48–55. [PubMed: 21987471]
21. Gerlach M, Ben-Shachar D, Riederer P, Youdim MB. Altered brain metabolism of iron as a cause of neurodegenerative diseases? Journal of neurochemistry. 1994; 63:793–807. [PubMed: 7519659]
22. Liu T, Eskreis-Winkler S, Schweitzer AD, Chen W, Kaplitt MG, Tsiouris AJ, Wang Y. Improved subthalamic nucleus depiction with quantitative susceptibility mapping. Radiology. 2013; 269:216–223. [PubMed: 23674786]
23. Liu C, Li W, Tong KA, Yeom KW, Kuzminski S. Susceptibility-weighted imaging and quantitative susceptibility mapping in the brain. Journal of magnetic resonance imaging : JMRI. 2014
24. Li W, Wu B, Liu C. Quantitative susceptibility mapping of human brain reflects spatial variation in tissue composition. Neuroimage. 2011; 55:1645–1656. [PubMed: 21224002]

25. Li W, Wu B, Batrachenko A, Bancroft-Wu V, Morey RA, Shashi V, Langkammer C, De Bellis MD, Ropele S, Song AW, Liu C. Differential developmental trajectories of magnetic susceptibility in human brain gray and white matter over the lifespan. Hum Brain Mapp. 2014; 35:2698–2713. [PubMed: 24038837]
26. Deistung A, Schafer A, Schweser F, Biedermann U, Turner R, Reichenbach JR. Toward in vivo histology: a comparison of quantitative susceptibility mapping (QSM) with magnitude-, phase-, and R2*-imaging at ultra-high magnetic field strength. Neuroimage. 2013; 65:299–314. [PubMed: 23036448]
27. Langkammer C, Liu T, Khalil M, Enzinger C, Jehna M, Fuchs S, Fazekas F, Wang Y, Ropele S. Quantitative susceptibility mapping in multiple sclerosis. Radiology. 2013; 267:551–559. [PubMed: 23315661]
28. Chen W, Gauthier SA, Gupta A, Comunale J, Liu T, Wang S, Pei M, Pitt D, Wang Y. Quantitative susceptibility mapping of multiple sclerosis lesions at various ages. Radiology. 2014; 271:183–192. [PubMed: 24475808]
29. Acosta-Cabronero J, Williams GB, Cardenas-Blanco A, Arnold RJ, Lupson V, Nestor PJ. In vivo quantitative susceptibility mapping (QSM) in Alzheimer's disease. Plos One. 2013; 8:e81093. [PubMed: 24278382]
30. Barbosa JH, Santos AC, Tumas V, Liu M, Zheng W, Haacke EM, Salmon CE. Quantifying brain iron deposition in patients with Parkinson's disease using quantitative susceptibility mapping, R2 and R2. Magnetic resonance imaging. 2015; 33:559–565. [PubMed: 25721997]
31. Hughes AJ, Daniel SE, Kilford L, Lees AJ. Accuracy of clinical diagnosis of idiopathic Parkinson's disease: a clinico-pathological study of 100 cases. Journal of neurology, neurosurgery, and psychiatry. 1992; 55:181–184.
32. Hoehn MM, Yahr MD. Parkinsonism: onset, progression and mortality. Neurology. 1967; 17:427–442. [PubMed: 6067254]
33. Fahn S, Elton RL, Committee UD. Unified Parkinson's disease rating scale. Recent developments in Parkinson's disease. 1987; 2:153–163.
34. Chaudhuri KR, Martinez-Martin P. Quantitation of non-motor symptoms in Parkinson's disease. European journal of neurology : the official journal of the European Federation of Neurological Societies. 2008; 15(Suppl 2):2–7.
35. Chaudhuri KR, Martinez-Martin P, Schapira AH, Stocchi F, Sethi K, Odin P, Brown RG, Koller W, Barone P, MacPhee G, Kelly L, Rabey M, MacMahon D, Thomas S, Ondo W, Rye D, Forbes A, Tluk S, Dhawan V, Bowron A, Williams AJ, Olanow CW. International multicenter pilot study of the first comprehensive self-completed nonmotor symptoms questionnaire for Parkinson's disease: the NMSQuest study. Movement disorders : official journal of the Movement Disorder Society. 2006; 21:916–923. [PubMed: 16547944]
36. Kobal G, Hummel T, Sekinger B, Barz S, Roscher S, Wolf S. "Sniffin' sticks": screening of olfactory performance. Rhinology. 1996; 34:222–226. [PubMed: 9050101]
37. Kang GA, Bronstein JM, Masterman DL, Redelings M, Crum JA, Ritz B. Clinical characteristics in early Parkinson's disease in a central California population-based study. Movement disorders : official journal of the Movement Disorder Society. 2005; 20:1133–1142. [PubMed: 15954133]
38. Schiess MC, Zheng H, Soukup VM, Bonnen JG, Nauta HJ. Parkinson's disease subtypes: clinical classification and ventricular cerebrospinal fluid analysis. Parkinsonism Relat Disord. 2000; 6:69–76. [PubMed: 10699387]
39. Berardelli A, Wenning GK, Antonini A, Berg D, Bloem BR, Bonifati V, Brooks D, Burn DJ, Colosimo C, Fanciulli A, Ferreira J, Gasser T, Grandas F, Kanovsky P, Kostic V, Kulisevsky J, Oertel W, Poewe W, Reese JP, Relja M, Ruzicka E, Schrag A, Seppi K, Taba P, Vidailhet M. EFNS/MDS-ES/ENS [corrected] recommendations for the diagnosis of Parkinson's disease. European journal of neurology : the official journal of the European Federation of Neurological Societies. 2013; 20:16–34.
40. Armstrong MJ, Litvan I, Lang AE, Bak TH, Bhatia KP, Borroni B, Boxer AL, Dickson DW, Grossman M, Hallett M, Josephs KA, Kertesz A, Lee SE, Miller BL, Reich SG, Riley DE, Tolosa E, Troster AI, Vidailhet M, Weiner WJ. Criteria for the diagnosis of corticobasal degeneration. Neurology. 2013; 80:496–503. [PubMed: 23359374]

41. Gilman S, Wenning GK, Low PA, Brooks DJ, Mathias CJ, Trojanowski JQ, Wood NW, Colosimo C, Durr A, Fowler CJ, Kaufmann H, Klockgether T, Lees A, Poewe W, Quinn N, Revesz T, Robertson D, Sandroni P, Seppi K, Vidailhet M. Second consensus statement on the diagnosis of multiple system atrophy. Neurology. 2008; 71:670–676. [PubMed: 18725592]
42. Langley J, Zhao Q. Unwrapping magnetic resonance phase maps with Chebyshev polynomials. Magnetic resonance imaging. 2009; 27:1293–1301. [PubMed: 19574009]
43. Schweser F, Deistung A, Lehr BW, Reichenbach JR. Quantitative imaging of intrinsic magnetic tissue properties using MRI signal phase: an approach to in vivo brain iron metabolism? Neuroimage. 2011; 54:2789–2807. [PubMed: 21040794]
44. Li W, Wang N, Yu F, Han H, Cao W, Romero R, Tantiwongkosi B, Duong TQ, Liu C. A method for estimating and removing streaking artifacts in quantitative susceptibility mapping. Neuroimage. 2015; 108:111–122. [PubMed: 25536496]
45. Li X, Vikram DS, Lim IA, Jones CK, Farrell JA, van Zijl PC. Mapping magnetic susceptibility anisotropies of white matter in vivo in the human brain at 7 T. Neuroimage. 2012; 62:314–330. [PubMed: 22561358]
46. Gattellaro G, Minati L, Grisoli M, Mariani C, Carella F, Osio M, Ciceri E, Albanese A, Bruzzone MG. White matter involvement in idiopathic Parkinson disease: a diffusion tensor imaging study. AJNR American journal of neuroradiology. 2009; 30:1222–1226. [PubMed: 19342541]
47. Ibarretxe-Bilbao N, Junque C, Marti MJ, Valldeoriola F, Vendrell P, Bargallo N, Zarei M, Tolosa E. Olfactory impairment in Parkinson's disease and white matter abnormalities in central olfactory areas: A voxel-based diffusion tensor imaging study. Movement disorders : official journal of the Movement Disorder Society. 2010; 25:1888–1894. [PubMed: 20669268]
48. Kundel HL, Polansky M. Measurement of observer agreement. Radiology. 2003; 228:303–308. [PubMed: 12819342]
49. Muenter MD, Tyce GM. L-dopa therapy of Parkinson's disease: plasma L-dopa concentration, therapeutic response, and side effects. Mayo Clinic proceedings. 1971; 46:231–239. [PubMed: 5573818]
50. Fahn S, Oakes D, Shoulson I, Kieburtz K, Rudolph A, Lang A, Olanow CW, Tanner C, Marek K. Levodopa and the progression of Parkinson's disease. The New England journal of medicine. 2004; 351:2498–2508. [PubMed: 15590952]
51. Paulus W, Jellinger K. The neuropathologic basis of different clinical subgroups of Parkinson's disease. J Neuropathol Exp Neurol. 1991; 50:743–755. [PubMed: 1748881]
52. Jellinger KA. Post mortem studies in Parkinson's disease--is it possible to detect brain areas for specific symptoms? Journal of neural transmission Supplementum. 1999; 56:1–29. [PubMed: 10370901]
53. Payoux P, Remy P, Damier P, Miloudi M, Loubinoux I, Pidoux B, Gaura V, Rascol O, Samson Y, Agid Y. Subthalamic nucleus stimulation reduces abnormal motor cortical overactivity in Parkinson disease. Archives of neurology. 2004; 61:1307–1313. [PubMed: 15313852]
54. Grafton ST, Turner RS, Desmurget M, Bakay R, Delong M, Vitek J, Crutcher M. Normalizing motor-related brain activity: subthalamic nucleus stimulation in Parkinson disease. Neurology. 2006; 66:1192–1199. [PubMed: 16636237]
55. Akakin A, Peris-Celda M, Kilic T, Seker A, Gutierrez-Martin A, Rhoton A Jr. The dentate nucleus and its projection system in the human cerebellum: the dentate nucleus microsurgical anatomical study. Neurosurgery. 2014; 74:401–424. discussion 424–405. [PubMed: 24448179]
56. Mure H, Hirano S, Tang CC, Isaias IU, Antonini A, Ma Y, Dhawan V, Eidelberg D. Parkinson's disease tremor-related metabolic network: characterization, progression, and treatment effects. Neuroimage. 2011; 54:1244–1253. [PubMed: 20851193]
57. Paris-Robidas S, Brochu E, Sintes M, Emond V, Bousquet M, Vandal M, Pilote M, Tremblay C, Di Paolo T, Rajput AH, Rajput A, Calon F. Defective dentate nucleus GABA receptors in essential tremor. Brain. 2012; 135:105–116. [PubMed: 22120148]
58. Wu T, Hallett M. A functional MRI study of automatic movements in patients with Parkinson's disease. Brain. 2005; 128:2250–2259. [PubMed: 15958505]
59. Yu H, Sternad D, Corcos DM, Vaillancourt DE. Role of hyperactive cerebellum and motor cortex in Parkinson's disease. Neuroimage. 2007; 35:222–233. [PubMed: 17223579]

60. Benarroch EE. Brain iron homeostasis and neurodegenerative disease. Neurology. 2009; 72:1436–1440. [PubMed: 19380704]

61. Lobel U, Schweser F, Nickel M, Deistung A, Grosse R, Hagel C, Fiehler J, Schulz A, Hartig M, Reichenbach JR, Kohlschutter A, Sedlacik J. Brain iron quantification by MRI in mitochondrial membrane protein-associated neurodegeneration under iron-chelating therapy. Annals of clinical and translational neurology. 2014; 1:1041–1046. [PubMed: 25574478]

62. Sedlacik J, Boelmans K, Lobel U, Holst B, Siemonsen S, Fiehler J. Reversible, irreversible and effective transverse relaxation rates in normal aging brain at 3T. Neuroimage. 2014; 84:1032–1041. [PubMed: 24004692]

63. Zucca FA, Segura-Aguilar J, Ferrari E, Munoz P, Paris I, Sulzer D, Sarna T, Casella L, Zecca L. Interactions of iron, dopamine and neuromelanin pathways in brain aging and Parkinson's disease. Prog Neurobiol. 2015

64. Jellinger KA. Pathology of Parkinson's disease. Changes other than the nigrostriatal pathway. Molecular and chemical neuropathology / sponsored by the International Society for Neurochemistry and the World Federation of Neurology and research groups on neurochemistry and cerebrospinal fluid. 1991; 14:153–197.

65. Jellinger KA, Paulus W. Clinico-pathological correlations in Parkinson's disease. Clin Neurol Neurosurg. 1992; 94(Suppl):S86–88. [PubMed: 1320531]

66. Gupta D, Saini J, Kesavadas C, Sarma PS, Kishore A. Utility of susceptibility-weighted MRI in differentiating Parkinson's disease and atypical parkinsonism. Neuroradiology. 2010; 52:1087–1094. [PubMed: 20358367]

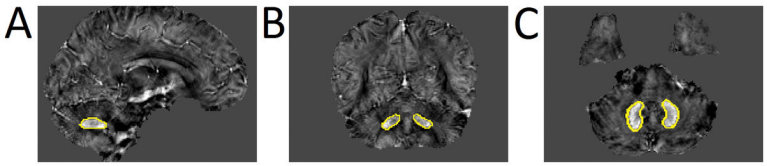

Figure 1.

A typical susceptibility map from one single patient with tremor dominant PD illustrates the positions of bilateral dentate nucleus.

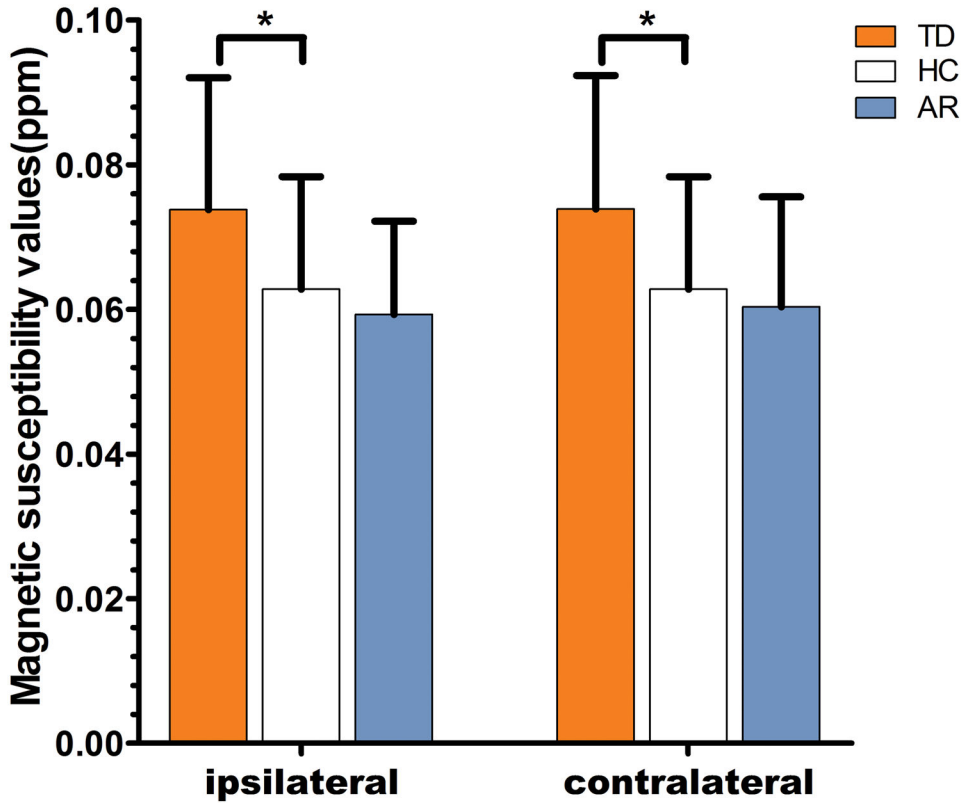

Figure 2.

Comparison of susceptibility values between ipsilateral or contralateral dentate nucleus in PD groups and pertinent mean values in bilateral sides of healthy controls, and Bonferroni correction was used for comparison between multiple groups. Significant differences between PD subgroups and control subjects are represented as: $^{*}p<.0167$.

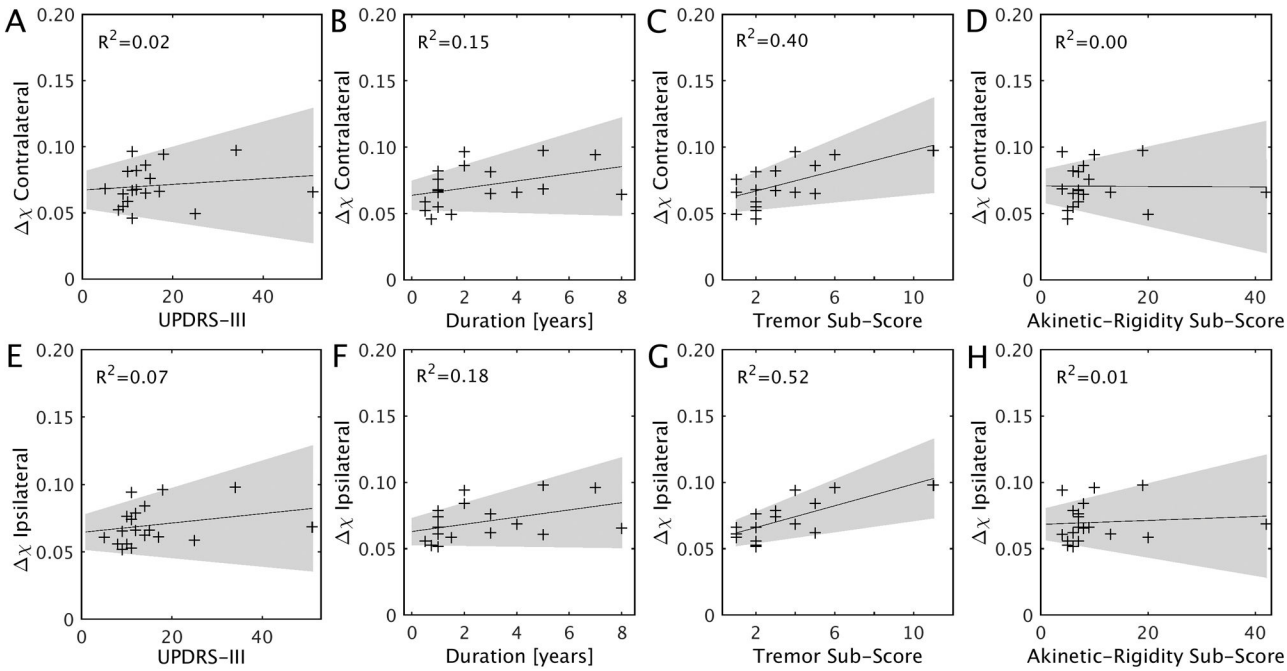

Figure 3.

Scatter plots and regression lines show the relationship between susceptibility values in bilateral DN and clinical measures in drug naive PD patients. The shaded region in each plot shows the 95% confidence interval. Correlations are partialed for gender, age, and education. P-value threshold for significance is 0.00357 adjusted based on Bonferroni correction.

Table 1

Demographic information and clinical characteristics of PD patients and healthy controls

Variable (mean±SD)	HC(*n*=48)	Overall PD (*n*=43)	TD (*n*=19)	AR (*n*=24)	*P* value
Gender(male/female)	21/27	19/24	8/11	11/13	0.812
Age(year)	61.7±6.5	63.7±6.9	62.7±8.2	64.5±5.9	0.426
Education(year)	11.1±3.5	11.8±3.5	12.2±3.3	11.5±4.2	0.552
MMSE	28.4±1.2	28.5±1.2	28.6±1.4	28.4±1.1	0.508
Disease Duration (year)	/	/	4.2±3.9	7.0±4.5	**0.038**
Hoehn and Yahr Scale	/	/	1.5±0.7	2.0±0.7	**0.023**
UPDRS-III score	/	/	16.1±7.3	26.8±13.1	**0.002**
Tremor score	/	/	3.8±2.2	1.1±1.4	**<0.001**
AR score	/	/	8.7±3.8	20.0±10.3	**<0.001**
NMS-Quest	/	/	3.6±3.3	7.3±4.7	**0.006**
ss-16	/	/	8.2±2.4	6.8±2.4	0.064

MMSE Mini Mental State Examination, UPDRS unified Parkinson's disease rating scale, TD tremor dominant, AR akinetic rigidity, HC healthy control, NMS non-motion symptom, ss-16 smell identification test from Sniffin'Sticks; Bold, p<0.05, significantly different between subgroups.

Table 2

Regional QSM values, R_2^* values, and volume of DN for patients with Parkinson's disease (PD) and healthy controls(HCs)

		TD *n=19*	HCs *n=48*	*P*	AR *n=24*	HCs *n=48*	*P*
QSM	ipsilateral	0.074±0.018	0.063±0.016	**0.016**	0.059±0.013	0.063±0.016	0.347
	contralateral	0.074±0.018		**0.015**	0.060±0.015		0.529
R_2^*	ipsilateral	32.0±5.5	29.1±5.0	0.055	27.7±5.8	29.1±5.0	0.299
	contralateral	32.7±8.4		0.099	29.7±5.1		0.631
Volume	ipsilateral	756.5±210.3	848.1±228.0	0.135	795.8±205.2	848.1±228.0	0.347
	contralateral	779.1±192.9		0.249	779.6±205.9		0.219

Data are presented as mean ±(SD); Bold, $p<0.025$, significantly different from controls after the Bonferroni correction; TD, tremor dominant Parkinson's disease; AR, akinetic rigidity dominant Parkinson's disease; HCs, healthy controls. Unit of QSM: ppm. Unit of R_2^* : s^{-1}. Unit of volume: pixels.

Table 3

Correlations between susceptibility values within bilateral DN with clinical features in drug naive PD patients

Clinical features	PD (*n*=19)	
	DN(ipsilateral)	DN(contralateral)
Disease Duration	0.338(0.200)	0.297(0.264)
UPDRS-III score	0.176(0.514)	0.091(0.736)
tremor score	**0.691(0.003)**	0.599(0.014)
AR score	0.003(0.990)	−0.071(0.793)
MMSE	−0.037(0.890)	0.001(0.997)
NMS-Quest	−0.128(0.637)	−0.194(0.471)
SS-16	0.144(0.594)	0.096(0.724)

Values are Pearson *r* correlation (*p* value), partialed for the effects of gender, age, and education, with multiple comparison corrections (Bonferroni correction). Bold, $p<0.00357$.